

Comfort Evaluation of the 'Católica' Pedestrian Bridge Based on SETRA 2006

Lenin Bendezu R.¹, Mathias Bazalar C.¹, Nayeli Rios M.¹, Malena Serrano²

¹Civil Engineering Department, Peruvian University of Applied Sciences
Av. General Salaverry 2255, Lima, Perú

²Florida International University, Miami, U.S.A.

pciplben@upc.edu.pe; u202124017@upc.edu.pe ; u20201b771@upc.edu.pe; mserr110@fiu.edu

Abstract – The increasing trend toward slender and low-stiffness pedestrian bridge designs has significantly raised their susceptibility to dynamic excitations induced by pedestrian activity. One of the most critical vibration phenomena in such structures is synchronous excitation, which occurs when the walking frequency of pedestrians coincides with the natural frequency of the bridge. This resonance condition can amplify the structural response, negatively impacting both user comfort and overall structural performance. These challenges are particularly relevant in densely populated urban environments such as Lima.

In this study, the dynamic behavior and comfort performance of the “Católica” pedestrian bridge were evaluated through in-situ vibration measurements using a geophone-based seismograph. The recorded data were analyzed based on the SETRA guideline, which classifies comfort into four levels according to peak vertical acceleration. This international reference was selected because, unlike the Peruvian bridge design standards—which do not explicitly consider pedestrian-induced vibrations as a dynamic load—the SETRA guideline has been applied in similar studies within the national context and offers more specific criteria for evaluating pedestrian comfort.

The results showed that vertical accelerations reached up to 0.541 g (5.31 m/s²) during pedestrian activity, corresponding to the lowest comfort level defined by the SETRA guideline. While most structural frequencies remained outside the resonance range, certain transverse modes during loading approached 1.2 Hz—a value close to the typical walking frequency range of pedestrians (1.7–2.3 Hz) suggesting a moderate potential for dynamic amplification. Although no clear resonance was detected, the elevated acceleration levels observed under normal use conditions highlight the need to implement vibration mitigation measures.

At this stage of the study, no single solution is prescribed. However, there is a recognized need to evaluate and compare various mitigation strategies in order to determine the most appropriate approach. These may include Tuned Mass Dampers (TMDs), damping pads, tuned stiffness elements, or minor structural modifications. A comparative assessment considering technical performance, ease of implementation, and cost-effectiveness would help identify the optimal solution. Such measures would allow the bridge to comply with the SETRA Level 1 comfort threshold (0.5 m/s²), thereby enhancing both safety and user comfort.

Keywords: Pedestrian-induced vibrations, Structural comfort, Bridge dynamics, Crowd synchronization, SETRA guideline

1. Introduction

Slender and low-stiffness pedestrian bridge designs are more prone to vibrations, especially due to synchronous excitation, which occurs when pedestrian walking frequency matches the bridge's natural frequency, amplifying vibrations and affecting comfort and safety.

This issue is particularly relevant in urban environments such as Lima. For example, [5] modeled the dynamic behavior of the “Rayito de Sol” footbridge using SAP 2000 and showed that even with damping mechanisms, vertical acceleration levels may exceed comfort thresholds. Similarly, [6] found a direct correlation between increased pedestrian density and greater structural acceleration in local footbridges. According to [7], walking frequencies typically range from 1.7 to 2.3 Hz and can reach up to 3.2 Hz when running—values that often match the natural frequencies of lightweight structures.

Despite advances in dynamic analysis tools, many studies still use fixed structural and walking parameters, limiting their accuracy under real-world variability. For instance, SAP2000 modeling of the Los Próceres bridge accurately estimated natural frequencies but did not reflect the diversity in pedestrian behavior. [4]

Recent research highlights the limitations of static and deterministic approaches. [8] showed that the efficiency of tuned mass dampers (TMDs) can drop by up to 20% under highly variable pedestrian flows. Meanwhile, [9] proposed treating pedestrians as dynamic systems, which resulted in over 30% reduction in vibrations—demonstrating the need for more realistic modeling strategies.

In response to these challenges, the present study evaluates the dynamic comfort of the *Católica* pedestrian bridge through a dual methodology. On one hand, real vibration data was collected using a geophone-based seismograph under actual pedestrian loading. On the other, pedestrian-induced loads were modeled in SAP2000 using crowd dynamics parameters from the literature. The measured data was then compared against comfort thresholds established by SETRA to validate the model and assess user comfort under real pedestrian flow conditions.

2. International Guidelines for Pedestrian Comfort

The dynamic behavior of pedestrian bridges under pedestrian loading is a key concern in structural design and assessment. To address this issue, various international guidelines have been developed to evaluate pedestrian-induced vibrations and ensure adequate comfort levels for users. Among them, the SETRA (2006) and HIVOSS (2008) guidelines stand out. In the present study, the analysis focuses exclusively on the criteria established by the SETRA (2006) guideline, due to its applicability to lightweight footbridges and its explicit emphasis on the relationship between acceleration, structural frequency, and comfort perception.

2.1. SETRA Guideline (2006)

The SETRA technical guideline (2006), developed by the French “Service d’Études Techniques des Routes et Autoroutes,” provides comprehensive criteria for assessing pedestrian comfort in footbridges subjected to vibrations induced by walking loads. This document is grounded in experimental investigations on human perception thresholds and the dynamic behavior of lightweight pedestrian structures, defining admissible acceleration and frequency ranges to prevent resonance effects and discomfort [1].

Pedestrian comfort is categorized into four levels according to the SETRA guideline [1], based on the maximum acceleration experienced by the structure in the vertical and longitudinal directions. Range 1 denotes a condition of *maximum comfort*, typically associated with very low levels of structural vibration. Range 2 corresponds to an *average comfort level*, generally acceptable for most users. Range 3 defines the *minimum tolerable comfort*, where vibrations may become more noticeable. Finally, Range 4 indicates an *unacceptable level of comfort*, where acceleration levels are considered too high for pedestrian use [1].

Table 1: Classification of Pedestrian Comfort Based on Vertical Acceleration Levels

Confort Level	0 – 0.5	0.5 – 1.0	1.0 – 2.5	2.5<
Range 1	Max			
Range 2		Mean		
Range 3			Min	
Range 4				Uncomfortable

Note: SETRA source.

Table 2: Classification of Pedestrian Comfort Based on Horizontal Acceleration Levels

Confort Level	0 – 0.15	0.15 – 0.30	0.30 – 0.8	0.8<
Range 1	Max			
Range 2		Mean		
Range 3			Min	
Range 4				Uncomfortable

Note: SETRA source.

In addition to structural accelerations, the SETRA (2006) guideline introduces a classification of natural frequencies in both the vertical and horizontal directions, corresponding to four distinct ranges associated with decreasing levels of resonance risk. Range 1 includes frequencies highly susceptible to resonance and should be avoided in design. Range 2 represents a moderate risk zone, where resonance effects may still be significant. Range 3 indicates a low risk of resonance, and Range 4 corresponds to frequencies where resonance is considered negligible. Based on this

classification, SETRA developed reference tables: Table 3 relates frequency ranges to vertical and longitudinal vibrations, while Table 4 applies the same concept to transverse vibrations. These tables provide a practical tool for evaluating whether a footbridge’s dynamic behavior under pedestrian loads falls within zones of concern regarding resonance effects, thereby supporting more robust assessments of structural comfort and safety [1].

Table 3:Frequency ranges (Hz) of the vertical and longitudinal vibrations

Frequency	< 1.0	1.0 – 1.7	1.7 – 2.1	2.1 – 2.6	2.6 – 5.0	5<
Range 1						
Range 2						
Range 3						
Range 4						

Note: SETRA source.

Table 4: Frequency ranges (Hz) of the transverse horizontal vibrations

Frequency	< 0.3	0.3 – 0.5	0.5 – 1.1	1.1 – 1.3	1.3 – 2.5	2.5<
Range 1						
Range 2						
Range 3						
Range 4						

Note: SETRA source.

2.2. Structural Resonance under Harmonic Excitation

When a pedestrian bridge is subjected to a periodic load whose frequency matches the structure’s natural frequency, a phenomenon known as resonance occurs. This condition causes a notable amplification of the structural response, even under low-magnitude loads. In pedestrian structures, such excitation typically originates from synchronized walking or crowd movements. This behavior, as discussed in the Sétra technical guide on dynamic behavior of footbridges [1], can be analytically described using a single-degree-of-freedom (SDOF) model. The governing equation of a single-degree-of-freedom (SDOF) damped oscillator (1), and simplifying, yields the frequency response function:

$$H_{x,F}(\omega) = \frac{X(\omega)}{\frac{F_0}{m}} = \frac{1}{\sqrt{(1 - \Omega^2)^2 + (2\xi\Omega)^2}} \tag{1}$$

Here, $H_{x,F}(\omega)$ is the transfer function relating the excitation force to the displacement response, m is the structural mass, $\Omega = \frac{\omega}{\omega_0}$ (2) is the frequency ratio between excitation and natural frequency ω_0 , and ξ is the damping ratio, a dimensionless quantity that describes how quickly oscillations decay. The dynamic amplification reaches its maximum near the resonance frequency Ω_R , defined as:

$$\Omega_R = \sqrt{1 - 2\xi^2} \tag{2}$$

At this point, the corresponding peak amplification is given by:

$$A(\Omega_R) = \frac{1}{2\xi\sqrt{1-\xi^2}} \quad (3)$$

This expression shows that lower damping ratios lead to higher amplification at resonance. For instance, if $\xi = 0.005$, the amplification factor may exceed 100, emphasizing the importance of damping in the structural design of pedestrian bridges. This theoretical behavior is illustrated in Figure 1.3 [1], which plots the amplification function $A(\Omega)$ across a range of excitation frequencies. The curve demonstrates how damping affects the amplitude of response, with the resonance peak becoming more pronounced as ξ decreases [1].

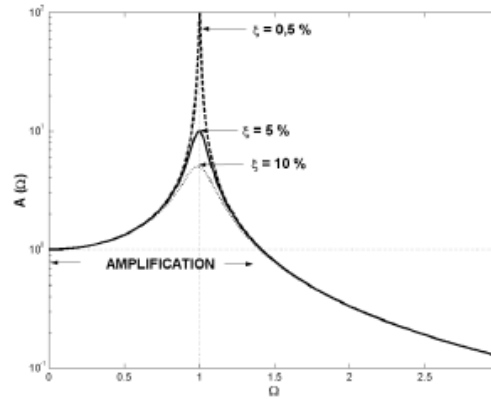


Figure 1: Resonance phenomenon

3. Field Test Using a Seismograph on the PUCP Pedestrian Bridge

To assess the dynamic behavior of the pedestrian bridge, on-site tests were conducted. The objective was to record the vibratory response of the bridge under ambient and pedestrian loading conditions, and to compare the results with the acceleration and frequency thresholds established by the SETRA guideline.

The measurement campaign was divided into two phases conducted on different dates. The first phase, an ambient vibration test, took place on Saturday, May 17, when foot traffic was minimal, allowing the structure's natural behavior to be recorded. The second phase was carried out on Tuesday, May 20, during exam week at the Pontifical Catholic University of Peru, taking advantage of increased pedestrian flow to evaluate the bridge under a representative dynamic load.

During the ambient vibration test, each measurement lasted one minute and was repeated at the three designated points along the bridge walkway. These data enabled the identification of the natural frequencies of the structure through spectral analysis of the recorded velocity signals. The execution of the ambient vibration test is documented in Figure 2.



Figure 2: ambient vibration test

The second phase, corresponding to the test under pedestrian loading, involved organizing groups of people at both ends of the bridge. Once data acquisition began, the participants were instructed to cross synchronously, generating a continuous and controlled dynamic load on the structure. Each recording also lasted one minute, resulting in a total of 36,000 records per point, considering the sampling interval of 1/600 seconds. The results of the second test are shown in Figure 3.



Figure 3: test under pedestrian loading

Using the velocity data obtained under both conditions, structural accelerations were calculated through numerical differentiation with respect to time. These accelerations were then compared with the comfort thresholds and resonance ranges defined by the SETRA guideline, in order to evaluate whether the bridge is at risk of vibration-related issues under real-use pedestrian traffic conditions.

4. Results

Each test had a total duration of one minute, during which 36,000 data samples per sensor were recorded. This corresponds to a sampling frequency of 600 Hz. Based on this, the time interval between records and the timestamp for each sample was defined as:

$$\Delta t = \frac{1}{600} = 0.0016667 \text{ s} \quad (6)$$

$$t_{n+1} = t_n + \Delta t \quad (7)$$

4.1. Conversion of Units: From Counts to Velocity

The raw records retrieved from the seismograph were stored in digital format (counts), which required conversion to physical units to allow for structural analysis [2]. This transformation considered the complete acquisition chain of the equipment, which includes a 4.5 Hz geophone sensor, a signal conditioning system, and a 24-bit sigma-delta ADC with an input range of ± 2.5 V. While the theoretical value of volts per count is:

$$\frac{\text{Volt}}{\text{count}_{\text{theoretical}}} = \frac{5 \text{ V}}{2^{24}} = 2.98 \times 10^{-7} \frac{\text{V}}{\text{count}} \quad (9)$$

Accordingly, the recorded counts were converted to velocity in m/s using the formula 9, where $S_g = 28.8 \text{ V/(m/s)}$ is the sensitivity of the geophone sensor.

$$v\left(\frac{\text{m}}{\text{s}}\right) = \frac{\text{Counts} \times \text{Volt/count}}{S_g} \quad (10)$$

4.2. Calculation of Structural Acceleration

The structural acceleration was computed using the velocity data by applying a first-order finite difference approximation between successive records. Subsequently, the acceleration was converted from m/s^2 to units of gravitational acceleration (g) using the standard value of gravitational acceleration. This process was applied to all three directions, enabling the analysis of vertical, longitudinal, and transverse accelerations.

$$a_n(\text{g}) = \frac{v_n - v_{n-1}}{\Delta t} \quad (11)$$

$$a_n(\text{g}) = \frac{a_n(\text{m/s}^2)}{9.80665} \quad (12)$$

4.3. Calculation of Structural Acceleration

Once the raw data from the five test points were converted into physical acceleration values, the processed files were analyzed using SeismoSignal. This software extracted key dynamic parameters—maximum acceleration, velocity, displacement, and predominant period—in the vertical (Z), transverse (N), and longitudinal (E) directions. As a representative case, the results from point 3, located at the mid-span of the central span, are shown in Figure 4, illustrating the time histories of displacement, velocity, and acceleration with clearly identifiable peaks.

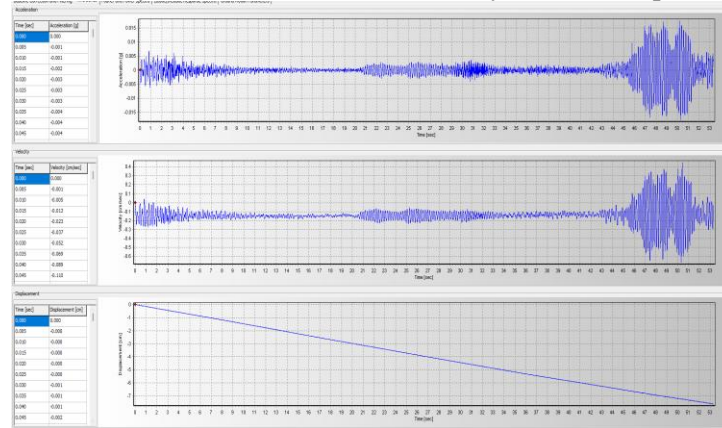


Figure 4: the time histories of displacement, velocity, and acceleration on point 3.

Following the individual analysis of the three measurement points located on the bridge deck, summary tables were compiled for each, presenting the maximum values and characteristic dynamic parameters. These tables distinguish between ambient conditions and pedestrian-loaded tests, enabling a direct comparison between the two operational scenarios. To characterize the structural behavior at Point 1, the acceleration values initially obtained in **g** were converted to **cm/s²** using the factor 1 g = 981 cm/s². With both peak acceleration and displacement values expressed in consistent units, the circular frequency ω (rad/s) was calculated using the following equation:

$$\omega = \sqrt{\frac{a_{max}}{d_{max}}} \quad (14)$$

Assuming a simple harmonic motion behavior, this enabled the estimation of the natural period T and frequency f using the standard relationships. This procedure was independently applied to the vertical, longitudinal, and transverse directions based on the processed signals from SeismoSignal.

Table 5: Point 1 under two different loading conditions.

Condition	Direction	Period (s)	Frequency (Hz)	Amax (g)	Amax(m/s2)
Ambient vibration	Vertical	3.291	0.304	0.041	0.402
	Lateral	4.933	0.203	0.025	0.245
	Transversal	5.120	0.195	0.037	0.363
Pedestrian flow	Vertical	6.447	0.155	0.337	3.306
	Lateral	4.297	0.233	0.090	0.883
	Transversal	2.933	0.341	0.089	0.873

Note: Own source.

Table 6: Point 2 under two different loading conditions

Condition	Direction	Period (s)	Frequency (Hz)	Amax (g)	Amax(m/s2)
Ambient vibration	Vertical	5.653	0.177	0.088	0.863
	Lateral	8.399	0.119	0.054	0.530
	Transversal	2.081	0.481	0.090	0.883
Pedestrian flow	Vertical	1.023	0.978	0.439	4.307
	Lateral	5.760	0.174	0.04	0.922
	Transversal	0.856	1.169	0.105	1.030

Note: Own source.

Table 7: Point 3 under two different loading conditions

Condition	Direction	Period (s)	Frequency (Hz)	Amax (g)	Amax(m/s2)
Ambient vibration	Vertical	4.257	0.235	0.044	0.432
	Lateral	7.181	0.139	0.015	0.147
	Transversal	1.249	0.801	0.016	0.157
Pedestrian flow	Vertical	2.228	0.449	0.541	5.307
	Lateral	1.503	0.665	0.140	1.373
	Transversal	0.817	1.223	0.142	1.393

Note: Own source.

5. Conclusion

This study evaluated the dynamic response and comfort performance of the “Católica” pedestrian bridge through in-situ structural measurements conducted under ambient vibration conditions and during pedestrian traffic. The signals were processed using a sensitivity of 2.98×10^{-7} V/count.

During the analysis, vertical accelerations of up to 0.541 g (5.31 m/s^2) were recorded under pedestrian loading, corresponding to Range 4 of the SETRA guideline, defined as an unacceptable level of acceleration for pedestrian structures. Regarding structural frequencies, most values remained within Range 4, which represents a negligible risk of resonance under ambient conditions. However, frequencies within Range 2 (1.6–2.4 Hz) were identified in the transverse direction at Points 2 (1.169 Hz) and 3 (1.223 Hz) during pedestrian passage, representing a moderate risk. Nevertheless, when these values were compared with those obtained under ambient conditions, no significant match was observed. Specifically, the resonance condition defined by SETRA was not satisfied, as it requires the loaded frequency to coincide with or closely match the natural unloaded frequency.

Given these findings, it is concluded that although no clear structural resonance was identified, the bridge exhibits vibration levels that exceed acceptable comfort thresholds during regular pedestrian use. Therefore, it is necessary to implement mitigation strategies to improve pedestrian comfort. However, at this stage of the study, no single solution is definitively proposed. Instead, it is recognized that several alternatives should be evaluated and compared before a final recommendation is made. These alternatives may include Tuned Mass Dampers (TMDs), damping pads, tuned stiffness elements, or even minor structural modifications. A comparative assessment considering effectiveness, technical feasibility, and cost would help determine the most suitable option for this particular case.

Acknowledgements

The authors would like to acknowledge the technical assistance provided by *IGR Ingenieros Consultores SAC* during the experimental campaign on the pedestrian bridge. Special thanks are extended to engineer Jorge Olarte for his support in the on-site vibration tests using the SARA seismograph, which was essential for the acquisition of high-quality dynamic data. The measurements and recommendations offered by IGR greatly contributed to the reliability and completeness of this research.

References

- [1] SETRA, *Assessment of Vibrational Behaviour of Footbridges under Pedestrian Loading*. Technical Guide, Service d'Études Techniques des Routes et Autoroutes, France, 2006.
- [2] DSN, IRIS & USGS, *Standard for the Exchange of Earthquake Data – Reference Manual*, Version 2.4, 2012.
- [3] Y. Liu and Z. Zhang, “Tuned mass damper with adjustable mass, stiffness and damping for bridge vibration reduction,” China Patent CN212957069U, Feb. 5, 2021
- [4] K. Loa, “Control de la respuesta dinámica en el puente peatonal los próceres mediante la incorporación de amortiguadores viscosos y de masa sintonizada”, Tesis de Maestría, Pontificia Universidad Católica del Perú, Lima, Perú, 2022.
- [5] G. Huaco and L. Vasquez, "Synchronic Excitation in Footbridges due Human-Induced Forces in Lima Peru," *IOP Conference Series: Materials Science and Engineering*, vol. 473, no. 1, pp. 06-09, 2019.
- [6] J. León, C. Melchor, and V. Sanchez, "Estudio del fenómeno de excitación sincrónica lateral: caso Puente Peatonal 'Rayitos de Sol'," *TECNIA*, vol. 30, no. 2, pp. 18–26, 2020.
- [7] I. Huergo-Ríos and H. Hernández, "Control pasivo de vibraciones verticales inducidas por personas en puentes peatonales," *Ingeniería Investigación y Tecnología*, vol. 21, no. 2, pp. 1–14, 2020.
- [8] F. Rezende, O. Brunet, W. Diniz Varela, A. Pereira, y E. Carvalho, “Evaluation of TMD performance in footbridges using human walking probabilistic models,” *Vibration*, vol. 4, no. 2, pp. 323–340, 2021.
- [9] P. Hawryszków, R. Pimentel, R. Silva y F. Silva, “Vertical vibrations of footbridges due to group loading: Effect of pedestrian–structure interaction,” *Applied Sciences*, vol. 11, no. 4, pp. 1–16, 2021.